A Classical Point Charge Model Study of System Size Dependence of Oxidation and Reorganization Free Energies in Aqueous Solution†

Regla Ayala and Michiel Sprik*

Department of Chemistry, University of Cambridge, Cambridge CB2 1EW, United Kingdom

Received: June 21, 2007; In Final Form: September 12, 2007

The response of water to a change of charge of a solvated ion is, to a good approximation, linear for the type of iron-like ions frequently used as a model system in classical force field studies of electron transfer. Free energies for such systems can be directly calculated from average vertical energy gaps. Exploiting this feature, we have computed the free energy and the reorganization energy of the M^{2+}/M^{3+} and M^{1+}/M^{2+} oxidations in a series of model systems all containing a single M^{n+} ion and an increasing number of simple point charge water molecules. Long-range interactions are taken into account by Ewald summation methods. Our calculations confirm the observation made by Hummer, Pratt, and Garcia (*J. Phys. Chem.* **1996**, *100*, 1206) that the finite size correction to the estimate of solvation energy (and hence oxidation free energy) in such a setup is effectively proportional to the inverse third power ($1/L^3$) of the length L of the periodic cell. The finite size correction to the reorganization energy is found to scale with $1/L$. These simulation results are analyzed using a periodic generalization of the Born cavity model for solvation, yielding three different estimates of the cavity radius, namely, from the infinite system size extrapolation of oxidation free energy and reorganization energy, and from the slope of the linear dependence of oxidation free energy on $1/L^3$. The cavity radius for the reorganization energy is found to be significantly larger compared to the radius for the oxidation (solvation) free energy. The radius controlling the $1/L^3$ dependence of oxidation free energy is found to be comparable to the radius for reorganization. The implication of these results for density functional theory-based ab initio molecular dynamics calculation of redox potentials is discussed.

1. Introduction

Polar solvents are capable of stabilizing ionic species that, in the gas-phase, only exist as short-lived transients, if at all. As a consequence, reactions changing the charge of solvated species (redox reactions) are accompanied by significant solvent reorganization, to the point that the reaction coordinate can be dominated by the solvent. Under these conditions, the reaction occurs only during certain favorable fluctuations of the solvent. These fluctuations are rare, and thus activated, even at the transition state geometry of the redox solutes. This phenomenon, often called nonequilibrium solvation,[1,2] was recognized by Marcus to be the key factor determining the reaction rate of outer-sphere electron transfer (ET) reactions in solution.[3−8] The order parameter quantifying the nonequilibrium solvation is the solvent reorganization energy. In the original formulation of his theory, Marcus treated the solvent as a linear dielectric continuum.[3,4] He introduced continuum polarization as an explicit independent degree of freedom that could deviate from its equilibrium value dictated by the charge and structure of the solute. Applied to an outer-sphere ET reaction ($D + A \rightarrow D^+ + A^-$) between a donor (D) and acceptor (A) species, this leads to the famous continuum expression for the reorganization energy[3]

$$\lambda = (\Delta q)^2\left(\frac{1}{\epsilon_{op}} - \frac{1}{\epsilon_{st}}\right)\left(\frac{1}{2R_D} + \frac{1}{2R_A} - \frac{1}{R_{DA}}\right) \qquad (1)$$

where R_D and R_A are the effective solvation (Born) radii of the donor and acceptor, respectively, and R_{DA} is their distance. ϵ_{op} is the high frequency (optical), and ϵ_{st} is the static dielectric constant of the solvent. Δq is the quantity of charge transferred (so $\Delta q = 1$ for elementary charge-transfer reactions). Equation 1 is one of the most intriguing results of continuum theory, and the conditions for its validity and possible generalization have been analyzed by a number of authors.[9−16]

Marcus subsequently extended his approach to atomistic models of the solvent, giving the reorganization energy a rigorous statistical mechanical basis.[6] This formalism was adapted and developed by Warshel into a concise and efficient method for the molecular dynamics (MD) study of ET reactions.[17,18] The reaction free energy change ΔA and reorganization energy λ in this approach are computed directly from the average vertical (optical) ET energy ΔE_{vt} in the reactant state $R = D + A$ and product state $P = D^+ + A^-$:

$$\Delta A = \frac{1}{2}(\langle \Delta E_{vt}\rangle_R + \langle \Delta E_{vt}\rangle_P) \qquad (2)$$

$$\lambda = \frac{1}{2}(\langle \Delta E_{vt}\rangle_R - \langle \Delta E_{vt}\rangle_P) \qquad (3)$$

where the subscripted angular brackets $\langle \Delta E_{vt}\rangle_M$ denote averages of the vertical energy gap ΔE_{vt} over a trajectory in the reactant ($M = R$) or product state ($M = P$). Being an implementation of Marcus theory, eqs 2 and 3 assume that the solvent responds linearly to a redistribution of charge of the solute. Warshel's gap method can, however, be generalized to nonlinear solvent response,[19] such as might occur when ET induces substantial reorganization of the coordination shell of the redox partners. This approach has been the basis for most of the numerical simulation studies of homogeneous ET[18−31] and heterogeneous ET.[32−39]

† Part of the "James T. (Casey) Hynes Festschrift".

* To whom correspondence should be sent. E-mail: ms284@cam.ac.uk.

10.1021/jp0748516 CCC: $40.75 © 2008 American Chemical Society
Published on Web 11/10/2007

Vertical energy gaps are also well-defined quantities in electronic structure calculations, and the gap method can therefore also be applied for computation of the reaction and reorganization free energies using density functional theory (DFT)-based ab initio MD (AIMD) methods.[40] We have used this approach in a series of AIMD studies of redox half reactions $R \rightarrow O + e^-$.[41−49] The relevant vertical energy is defined as

$$\Delta E_{vt}(\mathbf{R}^N) = E_O(\mathbf{R}^N) - E_R(\mathbf{R}^N) \tag{4}$$

where $E_O(\mathbf{R}^N)$ and $E_R(\mathbf{R}^N)$ are the ground-state energies of the oxidized (O) and reduced (R) system, respectively, and $\mathbf{R}^N$ denotes the atomic coordinates. Equations 2 and 3 straightforwardly apply, with the reduced state playing the role of reactant (R = R), and the oxidized state playing the role of the product (P = O). The AIMD technique is implemented in our work on half reactions in a rather "orthodox" interpretation: Solvent and solute are treated at the same level of DFT electronic structure calculation. Model systems consist of a single redox active solute and 30 to 100 solvent molecules (so no counterions). Periodic boundary conditions are applied.

The preoccupation with half reactions is partly motivated by technical considerations imposed by the DFT method used for the electronic structure calculation in AIMD. The vertical energy gap of eq 4 is an ionization energy that can be obtained from ground-state energy calculations. The restriction to half reactions therefore avoids the well-known difficulties of DFT determination of the vertical excitation energies required in full ET reactions. Furthermore, half reaction energies can be added (subtracted) to give estimates of the reaction free energy of full reactions. We found that, for a subclass of systems, these computed reaction free energy changes are comparable to the standard reaction free energy changes listed in thermochemical tables compiled by the experimentalists. This claim may at first seem surprising in view of the minimal periodic model systems used in AIMD calculations. Moreover, the change in net charge of our systems, when undergoing a redox reaction, makes concerns about boundary and finite size effects especially serious. However, compared to the huge errors for the half reaction energies (in the order of eV's) the free energies of the full reactions we have investigated so far are in good agreement with experimental values (for a recent list, see, for example, ref 49). Differences for the aqueous reactions are on the order of 0.2 eV,[41,46−48,50] and, for the reactions in nonaqueous solvent, the accuracy is better than 0.1 eV.[44,45] All our model reactions, however, are of a special type: they are isocoulombic, meaning that reactant and product species carry the same charges. This can be expressed schematically as

$$X^{m+1} + Y^m \rightarrow X^m + Y^{m+1} \tag{5}$$

If the species X and Y also have approximately the same spatial dimension, they will look, from a distance, similar to the solvent and periodic image charges. The long-range contribution to the oxidation free energies will be similar as well and therefore cancel in the full reaction.

The thesis that the very modest model system sizes of AIMD simulations, under certain circumstances, are still sufficient to obtain a reasonable estimate of redox free energies of full reactions is consistent with the observations by Hummer, Pratt, and Garcia, made in classical (force field model-based) calculations of the solvation free energies of aqua ions.[51−54] Their model systems, similar to ours, also contain only a single ion without counterions. Long-range interactions are treated using the same Ewald summation methods as in our AIMD codes. The free energy of solvation is computed by a process of stepwise charging of the ion, and can be directly interpreted as the classical "point charge" limit of the free energy of oxidation or reduction, that is, the half reaction energy obtained by our AIMD approach. Varying the system size (the number of solvent molecules), Hummer et al. noticed that systems consisting of 30 H_2O molecules, so similar in size to the systems used in AIMD, already lead to nearly converged estimates of solvation free energy.

The results on finite size scaling of ion solvation energies by Hummer et al. have been verified and analyzed by several other groups.[55−61] The picture of the effect of periodic boundary conditions on solvation energies emerging from this body of work may at first seem somewhat counterintuitive because the solvation energies obtained using this scheme include interactions with the periodic images of the ion and the homogeneous background of countercharge. These interactions are artifacts of the simulation method, so one is inclined to try to correct for them. These types of corrections are common in calculations of formation energies of charged point defects in semiconductors and oxides (for example silicates) and have been studied in great detail by the computational solid-state physics community.[62−67] The leading term is the energy of a point charge in a cubic array of point charges and a compensating uniform charge distribution; the next term accounts for the finite size of the defect:

$$\Delta E = \frac{\xi_{EW} q^2}{2L} - \frac{2\pi q^2 \Delta^2}{3L^3} + O(L^{-5}) \tag{6}$$

where q is the net charge, L is the cell parameter, and ξ_{EW} is the corresponding Madelung constant ($\xi_{EW} = -2.837$ for a simple cubic array). Δ is an effective radius formally defined as the root of the spherical second moment of the (localized) excess charge distribution normalized to the total charge.[63] Equation 6 holds for a lattice of ions plus background in vacuum. What Hummer et al. showed is that, in the case of aqua ions, the slowly converging first L^{-1} term is almost completely screened by the polarization of the solvent to the extent that, in high dielectric solvents such as water, the system size dependence of the energy of the ion is effectively dominated by the second term, which scales with inverse volume. The computer simulation evidence for this behavior[51] was backed up later by an analysis of the scaling of a dielectric continuum model.[52] The model is essentially an extension of the Born cavity model to cubic periodic boundary conditions. The result is an expression similar to eq 6 with the L^{-1} term multiplied by $1/\epsilon$ and the width Δ in the L^{-3} term replaced by the cavity radius. The value of the numerical prefactor was initially estimated using numerical methods and later derived analytically by Hünenberger and McCammon[58] and found to be identical to the $2\pi/3$ of the Makov−Payne expression eq 6 (for more details, see section 2.3).

The objective of the present study is to make a link between the work on classical ion solvation in periodic systems and the Marcus method of redox half reactions as employed in our AIMD simulations. We use the same classical force fields methods as Hummer et al., but the model ions we have investigated are not the alkali and chloride ions used in the ion charging work, but the "iron-like" three- and two-valent aqua cations, which are the favorite model system in classical simulation of ET.[21,25,27,35,37] We consider the half reaction

$$M^{2+}(aq) \rightarrow M^{3+}(aq) + e^- \tag{7}$$

where M is an "iron-like" aqua ion, i.e., with an ionic radius similar to that of Fe^{3+}. As previous work on this "textbook" Marcus ion has shown, the solvent response to the 2/3+ change in charge is well within the linear regime. As observed in a number of classical model studies,[22,28] nonlinear reorganization of the solvent in response to a redox reaction is more prominent for ions with lower (absolute) charge. Therefore, for comparison, we have also studied the related reaction

$$M^{1+}(aq) \rightarrow M^{2+}(aq) + e^- \quad (8)$$

For simple point charge (SPC) models, the reaction free energy of the half reaction (eq 7 or 8) can be directly identified with the difference in solvation energy (see section 2.2). Therefore, what the study of the system of high charge ions (eq 7) gains us, in comparison to monovalent ions, is that computation of solvation free energy is much easier since we can now exploit the linear approximation (eq 2). Only two equilibrium trajectories are required: one in the oxidized state, and the other in the reduced state. This enables us to determine the solvation energy for a series of solvent systems of increasing size within an accuracy sufficient to confirm that the size correction to the oxidation free energy indeed scales effectively with the inverse volume as predicted by the Hummer/Hünenberger continuum model. The same analysis is then carried out for the reorganization energy computed using eq 3. Anticipating our results, we find that reorganization energy converges with system size as L^{-1}. This is again in accordance with the corresponding expression obtained for the cavity model. This expression, the equivalent of eq 1 for half reactions in a periodic array of cavities, is also derived in the paper. The leading correction term is, in fact, equal to the $1/L$ term of the Makov−Payne relation (eq 6) multiplied by the Pekar factor $(1/\epsilon_{op} - 1/\epsilon_{st})$ with q replaced by Δq as in eq 1.

The remainder of the paper is organized as follows: Section 2 gives a brief outline of the version of the Marcus theory of ET employed here and of a related thermodynamic integration scheme. Section 2 then continues with a more detailed discussion of the dielectric continuum model. Technical details concerning the MD simulations are given at the end of section 2. Verification that the systems considered comply with the Marcus approach are detailed in section 3. The results and their discussion are presented in section 4. Concluding remarks of the work are summarized in section 5.

2. Theory and Method

2.1. Marcus Theory and Linear Response Approximation. The central statistical mechanical quantity in the microscopic formulation of Marcus theory is the restricted partition function for the vertical energy gap ΔE_{vt} (eq 4)[17]

$$Q_M(\Delta E) = \Lambda^{-3N} \int d\mathbf{R}^N \exp[-E_M(\mathbf{R}^N)/k_BT]\delta[\Delta E_{vt}(\mathbf{R}^N) - \Delta E] \quad (9)$$

where $E_M(\mathbf{R}^N)$ is the potential energy surface of the reduced (M = R) and oxidized species (M = O). ΔE is the specific value of ΔE_{vt} selected by the Dirac delta function. Λ is the average thermal wavelength defined as $\Lambda^{-3N} = \Pi_j \lambda_j^{-3N_j}/N_j!$, with λ_j being the thermal wavelength $\lambda_j = h/\sqrt{2\pi m_j k_B T}$ of the N_j nuclei of species j, and N being the total number of nuclei. All relevant quantities can be formally derived from $Q_M(\Delta E)$. The basic argument has been presented in numerous papers in the vast literature on the subject (for a recent and excellent introduction, see ref 2). Here we recall the expression for the free energy function (potential of mean force) of an oxidation state

$$A_M(\Delta E) = -k_BT \ln Q_M(\Delta E) \quad (10)$$

and the corresponding total free energy

$$A_M = -k_BT \ln \int d\Delta E e^{-A_M(\Delta E)/k_BT} \quad (11)$$

The free energy change of the oxidation reaction is then written as

$$\Delta A = A_O - A_R \quad (12)$$

and the reorganization energies for oxidation and the reverse reaction (reduction) is written as

$$\lambda_O = A_O(\Delta E_R) - A_O(\Delta E_O)$$
$$\lambda_R = A_R(\Delta E_O) - A_R(\Delta E_R) \quad (13)$$

where ΔE_M is the equilibrium value of the energy gap in state M. λ_R and λ_O can be interpreted as the reorganization free energies for the forward and backward reactions.

The gap relation (eq 2) for the oxidation free energy is an approximation of the exact ΔA of eq 12. This approximation is valid in the limit of linear response of the solvent to a change of charge of the solute. Under these conditions, the fluctuations of the energy gap can be assumed to be Gaussian or, equivalently, the free energy function $A_M(\Delta E)$ of the eq 11 quadratic in ΔE. Strict linear response, in fact, imposes the more stringent requirement that the curvatures of the parabolic free energies of the two oxidation states, or equivalently the widths (second moments) of the Gaussian gap distributions, are the same. This identity, which at first may not seem obvious, can be rigorously demonstrated.[17,68] With these Gaussian properties as a premise, eq 2 can be derived following a number of alternative routes (we refer to the literature for more details). The implication for the reorganization in the linear regime is that λ_R and λ_O of eq 13 are the same and identical to the λ given in eq 3. Because of the inverse relation between Gaussian gap fluctuations and the second derivative of the corresponding parabolic free energy function, we therefore have

$$\sigma_R^2 = \sigma_O^2 = 2k_BT\lambda \quad (14)$$

where σ_M is the root-mean-square fluctuation (second moment) of the vertical energy gap in the oxidation state M = R, O, and λ is the mean difference of the vertical gap (eq 3). Equation 14 is a rather strong condition that, in practice, is used to validate linear response for a given model system.

2.2. Point Charge Models and Thermodynamic Integration. For classical point charge models, as employed in the present investigation (see section 2.4), the vertical energy gap can be related to the electrostatic potential acting on the ion. ΔE_{vt} is, according to the definition of eq 4, the difference of the total potential energies of an oxidized (M = O) and reduced species (M = R) at a given solvent configuration $\mathbf{R}^N$. The energy of the system containing species M can be expressed as the sum of long- and short-range interactions:

$$E(\mathbf{R}^N) = \sum_{I=1,J>I}^{N} \frac{q_I q_J}{R_{IJ}} + VdW(\mathbf{R}^N) \quad (15)$$

where R_{IJ} is the distance between atom I and J with point charges q_I and q_J, respectively. In turn, the long-range interactions can be split up into ion−solvent and solvent−solvent interactions:

$$E_M(\mathbf{R}^N) = \sum_{I=2}^{N} \frac{q_M q_I}{R_{MI}} + \sum_{I=2,J>I}^{N} \frac{q_I q_J}{R_{IJ}} + VdW(\mathbf{R}^N) \qquad (16)$$

where q_M is the charge on the (in our case) cation indicated by index M = R,O and I = 2,...N now labeling the interaction sites of the solvent. Oxidation states in a SPC model only differ in the value of the point charge of the ion, q_O and q_R, with $q_O = q_R + 1$. Subtracting E_O and E_R we obtain

$$\Delta E_{vt}(\mathbf{R}^N) = \sum_{I=2}^{N} \frac{q_I}{R_{MI}} \qquad (17)$$

Because atomic positions are fixed, all interactions are eliminated except those involving the charge of the redox active ion. Therefore, as implied by eq 17, the vertical gap can be identified with the electrostatic potential ϕ_M at the site of the ion. For finite systems, or aperiodic extended systems, ϕ_M can be equally written as a derivative of the total energy:

$$\phi_M(\mathbf{R}^N) = \frac{\partial E_M(\mathbf{R}^N)}{\partial q_M} \qquad (18)$$

The reason is that, for these systems, the total energy is linear in q_M. However, total energies in periodic systems are computed using Ewald summation. This includes an interaction of the ion with its periodic images. Moreover, our half reaction model systems even carry a net charge, which introduces a further nonlinearity due to the interaction with the neutralizing background, which also depends on q_M. As a result, the vertical energy gap ΔE_{vt} and the potential defined in eq 18 are no longer equal. Of course, we can continue thinking about the vertical gap in periodic systems as an electrostatic (Madelung) potential, which must, however, be distinguished from the derivative potential ϕ_M of eq 18.

Both the vertical gap ΔE_{vt} of eq 4 and the derivative potential ϕ_M of eq 18 can be used in a thermodynamic integration scheme for the determination of oxidation free energy. This is straightforward for ϕ_M because this quantity is, by definition, equal to the charge gradient of the total energy:

$$\Delta A = \int_{q_R}^{q_O} \mathrm{d}q \left\langle \frac{\partial E_q}{\partial q} \right\rangle_q = \int_{q_R}^{q_O} \mathrm{d}q \langle \phi_q \rangle_q \qquad (19)$$

Here, E_q is the generalization of the energy surface of eq 16 in which the charge q_M of the redox active ion can take fractional values $q_R \le q \le q_O$. ϕ_q is the corresponding potential according to eq 18. The subscript q appended to the brackets indicates that the expectation values must be evaluated by using the canonical ensemble defined by E_q. Equation 19 is the basis of the charge scaling schemes applied in a number of force field model calculations of the solvation free energies available in the literature.

The implementation of a thermodynamic integration scheme based on the vertical energy gap follows the free energy perturbation method introduced by Warshel for the computation of the free energy of charge-transfer reactions. Applying Kirkwood's coupling parameter method,[69] the potential energy surfaces of reactant and product are superimposed to give a bias or mapping potential interpolating between reactant and product. For our half reactions, this amounts to a bias potential of the form

$$E_\eta = (1-\eta)E_R + \eta E_O = E_R + \eta \Delta E_{vt} \qquad (20)$$

where η is the thermodynamic perturbation parameter. Differentiating the bias potential w.r.t. to this parameter yields the vertical energy gap, and thus we can compute the oxidation free energy by integrating w.r.t. η:

$$\Delta A = \int_0^1 \mathrm{d}\eta \left\langle \frac{\partial E_\eta}{\partial \eta} \right\rangle_\eta = \int_0^1 \mathrm{d}\eta \langle \Delta E_{vt} \rangle_\eta \qquad (21)$$

The subscripted brackets again denote a thermal average over the E_η surface.

For Coulombic systems without self-interactions, we can set $\phi_M = \Delta E_{vt}$, and hence the thermodynamic integrals of eqs 21 and 19 are identical, with the parameter η playing the role of fractional charge. For periodic systems, the integrands are, in principle, different (although the integrals must, of course, end up to be the same). In particular, the charges of the redox active species used in the evaluation of the electrostatic energies in eq 21 are the actual charges of the reduced and oxidized species and are therefore strictly integers. This may only be a point of formal interest in classical point charge models. In electronic structure calculation, this distinction is absolutely crucial. Wave function-based self-consistent field calculations only allow for integer numbers of electrons. In DFT, it is possible to specify the fractional occupation of molecular orbitals. This, however, requires the utmost caution and, for molecular systems, can lead to highly unrealistic structures and energies if standard density functionals are used (see, e.g., ref 70). Note also that, for systems for which $\langle \Delta E_{vt} \rangle_\eta$ is approximately linear in η, we can estimate the integral eq 21 by the mean of the end point values corresponding to the reduced and oxidized states, thus recovering the Marcus gap formula (eq 2) for the reaction free energy. The free energy perturbation method therefore provides the most direct route for derivation of eq 2.[17,19,24]

2.3. Dielectric Continuum Model. Dielectric continuum representations of the solvent have been surprisingly successful for estimation of solvation free energies of ions. The simplest example of such a model is the Born expression for the solvation free energy of a spherical ion with charge q and radius R surrounded by a homogeneous linear dielectric medium of permittivity ϵ. The idea of the analysis by Hummer[52] and Hünenberger[58] is to compare the Born energy of a periodic array of such embedded spherical ions to the energy of a single ion in an infinite dielectric continuum. In the variant of the Born model used in refs 52 and 58, the charge of the ion is concentrated in a point residing at the center of a cavity of radius R. The cavity is assigned an internal dielectric permittivity of unity (vacuum). The solvation free energy of the infinite nonperiodic model is equal to the classic Born expression (as an alternative to the derivation for a conducting sphere):

$$F_B(\epsilon) = -\frac{q^2}{2R}\left(1 - \frac{1}{\epsilon}\right) \qquad (22)$$

Equation 22 is the energy gained by charging the ion in the dielectric "solvent" and subtracting the (singular) self-energy in vacuum ($\epsilon = 1$). It is instructive to review the derivation of eq 22 using the formalism applied in ref 52 to obtain the

expression for the periodic extension. The charging energy $F(\epsilon)$ is written as

$$F(\epsilon) = \frac{q^2}{2}\xi(\epsilon) \tag{23}$$

where $\xi(\epsilon)$ is the potential at the site of the point charge due to the polarization of the solvent by a unit charge ($q = 1$):

$$\xi(\epsilon) = \lim_{r\to 0}\left[\phi(\mathbf{r}) - \frac{1}{r}\right] \tag{24}$$

As usual $r = |\mathbf{r}|$. The electrostatic potential $\phi(\mathbf{r})$ is the solution of a heterogeneous Poisson equation

$$\nabla[\epsilon(\mathbf{r})\nabla\phi(\mathbf{r})] = -4\pi\rho(\mathbf{r}) \tag{25}$$

with the dielectric function ϵ(r) representing the cavity

$$\epsilon(\mathbf{r}) = \begin{cases} 1 & \text{if } r \le R \\ \epsilon & \text{if } r > R \end{cases} \tag{26}$$

The charge distribution $\rho(\mathbf{r})$ equals a delta function in the infinite nonperiodic system, so we set $\rho(\mathbf{r}) = \delta(\mathbf{r})$. We further require that the potential vanishes at infinite distance:

$$\lim_{r\to\infty}\phi(\mathbf{r}) = 0 \tag{27}$$

The inhomogeneous Poisson problem can be solved by partitioning $\phi(\mathbf{r})$ in an inner ($r \le R$) potential $\phi_-(\mathbf{r})$ and outer ($r > R$) potential $\phi_+(\mathbf{r})$. The dielectric discontinuity of eq 26 is then translated into matching conditions at the boundary of the cavity:

$$\phi_+(\mathbf{r}) = \phi_-(\mathbf{r}) \text{ for } r = R \tag{28}$$

$$\frac{\partial}{\partial r}\phi_-(\mathbf{r}) = \epsilon\frac{\partial}{\partial r}\phi_+(\mathbf{r}) \text{ for } r = R \tag{29}$$

The derivative relation eq 29 is a consequence of the requirement of continuity of the Maxwell displacement field $D(\mathbf{r})$. Taking now $\phi_+(\mathbf{r}) = 1/(\epsilon r)$ and $\phi_-(\mathbf{r}) = C + 1/r$, where C is a constant, we have satisfied eqs 25, 27, and 29. The value of C is found by inserting it in eq 28, giving $C = -(1 - 1/\epsilon)/R$. Substitution in eq 24 yields

$$\xi_B(\epsilon) = C = -\frac{1}{R}\left(1 - \frac{1}{\epsilon}\right) \tag{30}$$

and, with eq 23, we recover the Born energy of eq 22.

In refs 52 and 58, this derivation is generalized to treat a point charge in a spherical cavity replicated according to a cubic lattice with period L. The cavity must fit completely in a periodic cell, and hence $R < L/2$. Moreover, the point charge is now neutralized by a uniform charge distribution of opposite sign. The charge distribution in the central cell (containing the origin) becomes

$$\rho(\mathbf{r}) = q\left[\delta(\mathbf{r}) - \frac{1}{L^3}\right] \tag{31}$$

To find the corresponding periodic solvation energy, Hummer followed the route sketched above, namely, solving the inhomogeneous Poisson eq 25 for $q = 1$ with the dielectric function in the cell given by eq 26. Adopting Ewald ("tin-foil") boundary conditions at infinity enabled him to compute the charging energy, as for the nonperiodic system, from eq 23 using eq 24 because, under these conditions, the average potential integrated over the cell volume $V = L^3$ vanishes:

$$\int_V d\mathbf{r}\phi(\mathbf{r}) = 0 \tag{32}$$

and, therefore, the potential energy of the background charge as well (to be distinguished from the contribution of the background to the potential, which is not zero). $\phi(\mathbf{r})$ can again be found by separating it into an inner and outer potential, and eqs 28 and 29 still apply. These conditions are supplemented by a relation ensuring periodicity of the potential in the cubic lattice

$$\frac{\partial}{\partial x}\phi_+(\mathbf{r}) = 0 \text{ for } x = \pm L/2 \tag{33}$$

with an analogous equation for the y and z coordinates. The boundary condition at infinity of eq 27 is, of course, no longer valid and is effectively replaced by eq 32.

The solution for the quantity $\xi(\epsilon)$ of eq 24 for the periodic system is, according to ref 58, given by

$$\xi_L(\epsilon) = \xi_B(\epsilon) + \frac{1}{L}\left[\frac{\xi_{EW}}{\epsilon} - \left(1 - \frac{1}{\epsilon}\right)\left(\frac{4\pi}{3}\left(\frac{R}{L}\right)^2 - \frac{16\pi^2}{45}\left(\frac{R}{L}\right)^5\right)\right] \tag{34}$$

where $\xi_B(\epsilon)$ is the nonperiodic Born potential of eq 30, and $\xi_{EW} = -2.837297$ is the Madelung constant of a cubic lattice. Terms of higher order in R/L have been neglected in eq 34, assuming that the cavity radius is small compared to the box length. Equation 34 was derived by Hünenberger and McCammon[58] from an analytical solution of the Poisson equation. The same result was obtained earlier by Hummer et al.[52] with the help of numerical methods (note, however, that the constant multiplying the $(R/L)^2$ term in ref 52 differs by a factor of 2 compared to eq 34; see ref 58). Substituting in eq 23, we find for the leading finite size correction to the energy

$$F_L(\epsilon) - F_B(\epsilon) = \frac{q^2\xi_{EW}}{2\epsilon L} - \left(1 - \frac{1}{\epsilon}\right)\frac{2\pi q^2 R^2}{3L^3} \tag{35}$$

We note immediately that, in the limit of infinite lattice parameter L, the energy of the periodic system $F_L(\epsilon)$ converges to the energy $F_B(\epsilon)$ of eq 22 for the nonperiodic system. A further limit of interest is an ion with vanishing radius R. While the Born energy for such a system diverges (for $\epsilon > 1$), the difference between the periodic and nonperiodic energy approaches a finite value: the Wigner energy of an array of point charges. This energy remains when the solvent is removed ($\epsilon = 1$). In the opposite limit of solvents with high dielectric constants such as water, this term will be small and, for system sizes accessible to simulation, can easily be dominated by the contribution of the second term in eq 35. This term, similar to the nonperiodic Born solvation energy, is for strongly polarizable solvents independent of ϵ.

Equation 35 is the central result of ref 52 lending theoretical support for the empirical observation made in previous[51] and subsequent work[53,54] that the hydration energy computed by Ewald summation is practically independent of system size for the models normally used in simulation (100 water molecules or more). Equation 35 coincides with the Makov−Payne expression (eq 6) in the absence of solvent ($\epsilon = 1$). What matters for the modeling of solvation is of course the $\epsilon > 1$ generaliza-

tion of eq 6. A common modification found in the literature (see, e.g., ref 66) is

$$\Delta E = \frac{q^2 \xi_{\mathrm{EW}}}{2\epsilon L} - \frac{2\pi q^2 \Delta^2}{3\epsilon L^3} + O(L^{-5}) \tag{36}$$

The first terms in eq 36 and eq 35 are identical. The crucial difference is in the ϵ dependence of the second term, which, in eq 36, is treated similarly to the first term. However, accounting for a dielectric response to charging of an ion is apparently not as straightforward as multiplication by an overall $1/\epsilon$. We refer to refs 64 and 65 for a more recent and consistent method for the computation of defect formation energies, which may well be compatible with the cavity approach.

The effective inverse volume dependence of solvation energy has been verified and discussed by a number of other workers,[55,56,59−61] and we expect this to hold for our oxidation free energies as well. Thus, using eq 35, we can write for the free energy of oxidation in the periodic system

$$\Delta A_L(\epsilon) - \Delta A_{\mathrm{B}}(\epsilon) = ({q_{\mathrm{O}}}^2 - {q_{\mathrm{R}}}^2)\left[\frac{\xi_{\mathrm{EW}}}{2\epsilon L} - \left(1 - \frac{1}{\epsilon}\right)\frac{2\pi R^2}{3L^3}\right] \tag{37}$$

where q_{O} and q_{R} are the charges of the ion in the oxidized and reduced states, respectively, and R is the effective spherical ion radius assumed to be the same for the two oxidation states. ΔA_{B} is the continuum (Born) model prediction for the oxidation free energy, which, according to eq 22, is given by

$$\Delta A_{\mathrm{B}} = -\frac{({q_{\mathrm{O}}}^2 - {q_{\mathrm{R}}}^2)}{2R}\left(1 - \frac{1}{\epsilon}\right) \tag{38}$$

Neglecting the small L^{-1} contribution, we therefore have for the effective system size dependence of the free energy

$$\Delta A_L \approx \Delta A_{\mathrm{B}} - ({q_{\mathrm{O}}}^2 - {q_{\mathrm{R}}}^2)\frac{2\pi R^2}{3L^3} \tag{39}$$

The question is now whether the reorganization energy shows a similar behavior. The reorganization energy λ as introduced by Marcus is, in principle, a nonequilibrium solvation energy. However, he also showed that, in the framework of dielectric continuum theory, λ can be estimated from equilibrium solvation energies evaluated at two different values of the dielectric constant, namely, the optical (high frequency) dielectric constant ϵ_{op}, describing the response of the electronic polarization of the system, and the static dielectric constant ϵ_{st}, which also includes the orientational (inertial) response of the permanent dipoles of the molecules. The result is eq 1, the expression starting off this paper. Note, however, that the equilibrium solvation energies concerned are not the energies of the charge distributions of the oxidized state ($\rho_{\mathrm{O}}(\mathbf{r})$) or reduced states ($\rho_{\mathrm{R}}(\mathbf{r})$), but of their difference $\Delta\rho(\mathbf{r}) = \rho_{\mathrm{O}}(\mathbf{r}) - \rho_{\mathrm{R}}(\mathbf{r})$. This makes an important difference because solvation energies are quadratic in the solute charge. In our SPC model, $\Delta\rho$ is given by eq 31 with q replaced by $\Delta q = q_{\mathrm{O}} - q_{\mathrm{R}}$:

$$\Delta\rho(\mathbf{r}) = \Delta q\left[\delta(\mathbf{r}) - \frac{1}{L^3}\right] \tag{40}$$

The continuum approximation for reorganization energy is often formulated in terms of integrals over the corresponding Maxwell displacement field $\mathbf{D}(\mathbf{r})$[4,9,10]:

$$\lambda = \frac{1}{8\pi}\int \mathrm{d}\mathbf{r}\left[\frac{|\mathbf{D}(\Delta\rho,\epsilon_{\mathrm{op}})|^2}{\epsilon_{\mathrm{op}}} - \frac{|\mathbf{D}(\Delta\rho,\epsilon_{\mathrm{st}})|^2}{\epsilon_{\mathrm{st}}}\right] \tag{41}$$

The spatial dependence of the displacement field has been suppressed in eq 41. Instead, we have highlighted the dependence on the external charge distribution, $\Delta\rho$, generating the field via the Maxwell equation

$$\nabla\cdot\mathbf{D}(\mathbf{r}) = 4\pi\Delta\rho(\mathbf{r}) \tag{42}$$

The second formal argument of the displacement field in eq 41 is the dielectric constant of the medium. While ϵ does not enter eq 42, the solution of eq 42 may indirectly depend on ϵ in more complex heterogeneous systems, as, for example, pointed out by Newton and Friedman[13,14](see also ref 16). For this reason, these authors make a strong argument in favor of using the alternative expression for λ in terms of integrals over potentials and charge distributions. In the notation introduced in eq 41, this expression as derived in ref 13 (see also ref 14) is written as

$$\lambda = \frac{1}{2}\int \mathrm{d}\mathbf{r}\Delta\rho[\phi(\Delta\rho, \epsilon_{\mathrm{op}}) - \phi(\Delta\rho,\epsilon_{\mathrm{st}})] \tag{43}$$

where $\phi(\mathbf{r})$ is obtained by solving the Poisson equation (eq 25) with $\Delta\rho(\mathbf{r})$ as the source term. Equation 43 is equivalent to the original expression by Marcus.[4] Equation 41 can be derived from eq 43 by partial integration. This is the critical step that may cause complications in periodic systems and is the reason why we prefer eq 43 over eq 41 in the present application. Since the charge distribution in extended systems is not confined to a domain in space, partial integration in general introduces surface terms, unless special symmetry surfaces are selected. However, we need not to worry about this in eq 43, where integration is over the full central cell. A second practical consideration is that, for point charge models, computation of the integral of eq 43 is easy, involving only the potential at the exact site of the ion. In fact, we can directly apply the approach used for solvation energies outlined above. The key quantity was the site (Madelung) potential $\xi(\epsilon)$ of eq 24. Thus, with eq 23, we find

$$\lambda = \frac{(\Delta q)^2}{2}[\xi(\Delta\rho, \epsilon_{\mathrm{op}}) - \xi(\Delta\rho, \epsilon_{\mathrm{st}})] \tag{44}$$

Inserting eq 30 yields the Marcus continuum approximation for the reorganization energy of an oxidation (half) reaction in an infinite medium:

$$\lambda_{\mathrm{B}} = \frac{(\Delta q)^2}{2R}\left(\frac{1}{\epsilon_{\mathrm{op}}} - \frac{1}{\epsilon_{\mathrm{st}}}\right) \tag{45}$$

where we have added a suffix B to be consistent with our notation introduced earlier. Substituting eq 34, we obtain the equivalent in cubic periodic systems:

$$\lambda_L = \lambda_{\mathrm{B}} + \frac{(\Delta q)^2}{2L}\left(\frac{1}{\epsilon_{\mathrm{op}}} - \frac{1}{\epsilon_{\mathrm{st}}}\right)\left[\xi_{\mathrm{EW}} + \frac{4\pi}{3}\left(\frac{R}{L}\right)^2 - \frac{16\pi^2}{45}\left(\frac{R}{L}\right)^5\right] \tag{46}$$

We see that, in contrast to the oxidation energy, the term proportional to $1/L$ is determined by the Wigner interaction

energy screened by the Pekar factor. Its value will, in general, exceed the $1/L^3$ term, which determined the finite size effect for the oxidation energy. The conclusion is that size corrections for reorganization energy are subject to the unfavorable inverse cell length scaling one would normally expect for coulomb interactions. Accordingly, the effect is independent of ion parameters except charge. The correction is always negative, leading to serious underestimation of λ, which is, however, identical for all one-electron redox reactions in a given solvent. Disregarding all higher order terms, we obtain the following simple continuum approximation for the reorganization energy for a half reaction under cubic periodic boundary conditions:

$$\lambda_L = \frac{(q_O - q_R)^2}{2}\left(\frac{1}{\epsilon_{op}} - \frac{1}{\epsilon_{st}}\right)\left(\frac{1}{R} + \frac{\xi_{EW}}{L}\right) \qquad (47)$$

where we have replaced Δq by its definition in order to emphasize the distinction with eq 39 for the oxidation free energy. In the nonpolarizable aqueous force field models considered here, $\epsilon_{op} = 1$ and $\epsilon_{st} = \epsilon \gg 1$, and the ϵ-dependent (Pekar) factor reduces to unity.

We conclude this section with a more theoretical comment on the relation between reorganization energy and oxidation free energy. Just as the disappearance of the $1/L$-dependent lattice contribution to ΔA is somewhat unexpected, so is its appearance in the correction to λ. Reorganization energy as defined in eq 13 represents a free energy of a nonequilibrium configuration of the solvent on a single diabatic energy surface. The interaction of the ion with its images and background is a constant on this surface and should not contribute to the reorganization energy. Viewed from the perspective of ET theory, one can say that Wigner lattice energy is a form of (spurious) electronic polarization, instantly responding to a change of charge of the solute, and therefore not part of the inertial polarization that constitutes the reorganization energy. An equivalent view, which is also the basis for the computation of reorganization energy in continuum theory,[4,9−14] is to equate λ to the net result of adiabatic charging (or ET) followed by vertical discharging. The second step eliminates the periodic self-interaction energy built up in the first step. This cancellation is perhaps most explicit in the linear approximation in eq 3 expressing reorganization energy as a difference of ionization energies.

The question is thus, how can there be a Wigner-like term in the reorganization energy if it is not due to self-interactions of a periodic array of ions plus background? This question can be answered in the framework of the hypothesis of Hummer et al.[52] about the response of a strongly polarizable medium in such a system. Their argument was that, in addition to the Wigner self-interaction energy, there is a further long-range contribution related to the periodic perturbation of the solvent structure. The water molecules in the cells adjacent to the central cell are oriented to solvate an image ion and are therefore in an unfavorable orientation for the interaction with the central ion and its solvation shells. This interaction energy is repulsive and, as Hummer et al. inferred, almost exactly compensates the overstabilization by the Wigner interaction. This self-energy term, however, is missing in the reorganization energy, leaving λ with the orientational mismatch of the solvent molecules, which is a purely inertial effect. With no self-interaction energy to balance it, this long-range effect now determines the finite size error in λ, exposing the effective $1/L$ scaling behavior of the inertial solvent polarization.

2.4. Model Systems and MD Method. In our classical description, the system is represented by a cubic box periodically replicated containing one metal ion solvated by explicit water molecules. The MD simulations were carried out at constant temperature (298 K) and fixed volume. We have investigated eight solvent model systems consisting of 17, 35, 43, 65, 121, 256, 512, and 1000 water molecules and a single metal ion. The length of the cubic cell was set so as to agree with the experimental density of the liquid water at 25 °C and 1 atm. This leads to cell lengths of $L = 7.820$ (17), 10.0 (35), 10.757 (43), 12.414 (65), 15.350 (121), 19.706 (256), 24.827 (512), and 31.034(1000) Å, where the numbers in brackets indicate the number of solvent molecules. For each of these model systems, we generated three trajectories, one for each of the three oxidation states of the cation (eqs 7 and 8).

It has been demonstrated[26] that, although a flexible model is needed when one is interested in the quantum effects on the ET reaction, the contribution of intramolecular vibration to the static reorganization free energy is quantitatively small. For this reason, an SPC rigid water model[71] was employed for the solvent interactions. The cations were described by a Lennard-Jones-type model developed by Ando for the $Fe^{2+/3+}$ aqua ion on the basis of ab initio calculations[27] and charges 1+, 2+, and 3+. The Lennard-Jones parameters for the ion−oxygen interaction we used are $\sigma = 2.639$ Å and $\epsilon = 0.0708$ kcal/mol (compared to $\sigma = 3.166$ Å and $\epsilon = 0.1554$ kcal/mol for the oxygen−oxygen interaction of the water model). The partial charge on the O site is $-0.82e$, and that on an hydrogen site is $+0.41e$. PBC were applied. The cutoff distance for the non-bonded interactions was L/2, with L being the box dimension. Long-range interaction corrections were incorporated by means of Ewald summation.[72] A time step of 1 fs was used. The thermalization period was between 10 and 40 ps. At least 2 ns of production runs were performed for each of the cations and size systems considered. Structures were saved every 10 ps for further analysis. The MD simulations were performed using the DL_POLY program.[73]

3. Results and Discussion

3.1. Validation of Linear Response Approximation. Prior to application of the Marcus energy gap relations (eqs 2 and 3) to the reactions in eqs 7 and 8, we verified whether the underlying linear response approximation is valid for these half reactions. As explained in section 2.2, evaluation of a vertical energy gap ΔE_{vt} for a classical point charge model is a straightforward task: simply subtract total energies obtained for two different values of the point charge of the cation ($q_O = 3$, $q_R = 2$ for reaction eq 7, and $q_O = 2$, $q_R = 1$ for reaction eq 8) for the same configuration of atomic positions generated by the MD simulations. This procedure was applied to the configurations saved in the production runs. A strict condition for the Marcus assumption of quadratic free energy surfaces to hold is that the variance of the fluctuations of ΔE_{vt} is independent of the oxidation state of the ion (eq 14). This test was carried out for one of the medium-sized model systems, namely, the system containing 121 water molecules. All three oxidation states (M^{n+}, $n = 1$, 2, and 3) were investigated. The results for the gaps of the M^{2+}/M^{3+} pair are shown in Figure 1, both in the form of the time series sampled from the trajectory and in the form of histograms. These histograms can be smoothly fitted to a Gaussian distribution, although some fluctuations can be observed. The width of the histograms for the 2+ and 3+ charge are the same (0.26 and 0.28 eV; see Figure 1) within our statistical accuracy, confirming the conclusions of previous studies of this model system, that the M^{2+}/M^{3+} pair, mimicking the aqueous ferrous/ferric ion couple, behaves as an almost

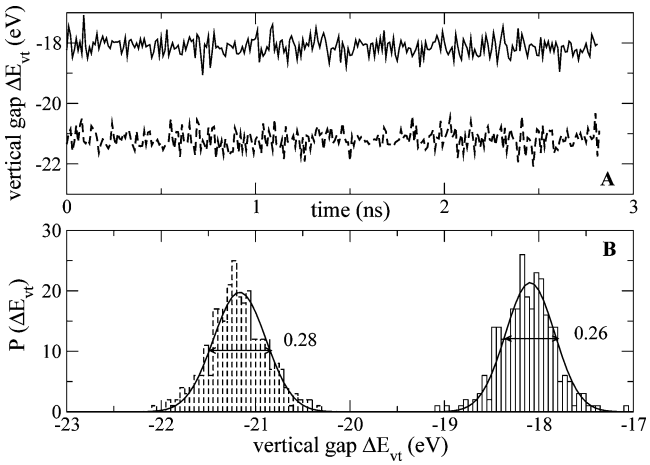

Figure 1. (A) Time evolution of the vertical energy gap ΔE_{vt} of M^{2+} (solid curve) and M^{3+} aqua cations (dotted curve) for a system containing 1 ion + 121 SPC water molecules. ΔE_{vt} is defined according to eq 4 as the change in total energy of a given (instantaneous) configuration of solvent and ion coordinates when the charge of the ion is changed from 2+ (reduced) to 3+ (oxidized). Periodic boundary conditions are applied. (B) Histograms of the ΔE_{vt} time series in panel A and Gaussian fit. The numbers indicate the width (root of the second moment) of the distributions.

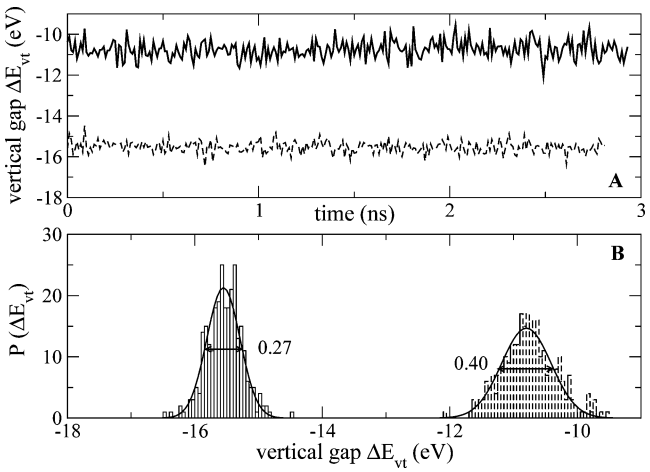

Figure 2. (A) Time evolution of the vertical energy gap ΔE_{vt} of the M^{1+} (solid curve) and M^{2+} aqua cations (dotted curve) of a 1 ion + 121 SPC water molecule model similar to the system used in Figure 1. ΔE_{vt} is now the difference in energy of the 2+ (oxidized) relative to the 1+ (reduced) charge state of the ion for an instantaneous configuration of solvent and ion coordinates. (B) Histograms of ΔE_{vt} fluctuations and Gaussian fit. The numbers indicate the width of the distributions.

perfect Marcus system. For the M^{1+}/M^{2+} pair (Figure 2), a similar procedure indicates that, although the histograms of ΔE_{vt} can be fitted to Gaussian distributions, their width shows a clear variation with oxidation state. The width of the fluctuations of the vertical oxidation potential of the reduced state M^{+1} is almost double (0.40 eV) the one for (minus) the vertical electron affinity of the oxidized state M^{2+} (0.27 eV). This discrepancy precludes, in principle, the use of eqs 2 and 3 in the case of the M^{1+}/M^{2+} pair. We see again, as already pointed out in refs 68 and 19, that a reasonably good Gaussian fit to the equilibrium energy gap fluctuations is a necessary but certainly not sufficient condition for linear solvent response (see also refs 22 and 23).

These results raise two questions: (1) What is the difference between reactions eq 7 and 8? and (2) If we apply the energy gap relations to the pair M^{1+}/M^{2+}, what is the error we make? To answer the first question, we determined the radial distribution for the $M^{n+}-O$ ($n = 1$, 2, and 3) distance. These structural data, displayed in Figure 3, suggest that the solvent reorganization accompanying the redox process is more severe in the case of the M^{1+}/M^{2+} pair than in the M^{2+}/M^{3+} pair. As expected, a decrease of the charge on the cation leads to an increase in the $M^{n+}-O$ distance. This effect is easily explained in terms of the elementary ion−water interaction potentials used in this study, in which the three cations have the same Lennard-Jones parameters. The large electrostatic attraction has pulled the oxygen atoms of the solvent well into the repulsive core of the short-range potential. Decreasing the charge will lower the ion−water electrostatic energy, and the solvent molecules will be pushed back, increasing the $M^{n+}-O$ distance. With regard to coordination numbers, the first hydration shell of the M^{2+} and M^{3+} ions consists of six water molecules at distances of 2.03 and 1.93 Å, respectively. These water molecules do not exchange with water molecules from more remote hydration shells during the simulation time. The hydration shell of M^{1+} is more fluxional: the number of water molecules directly coordinated to the ion fluctuates between five and six, the average being 5.3. Contrary to the cations of higher charge, exchange of water molecules in the first solvation shell can be observed on the time scale of the simulation. A change in coordination is presumably outside the linear response regime, which could also be the reason for the difference in width of the Gaussian distribution of ΔE_{vt} for the half reaction involving charges 1+ and 2+. Again we are not the first to note an increased tendency for nonlinear response of the solvent with decreasing solute charge. A similar discussion, for example, can be found in ref 28.

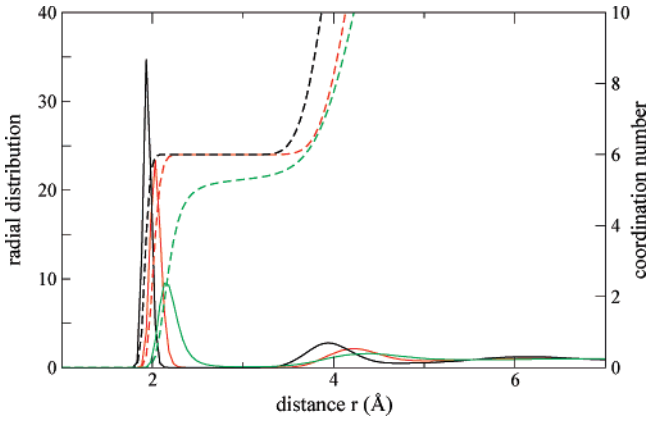

Figure 3. M^{n+}−oxygen ($n = 3$ (black), 2 (red), and 1 (green)) radial distribution functions and their running coordination numbers for the solvent + ion systems of Figures 1 and 2.

To answer the question to what extent these nonlinearities affect the redox free energies, we computed the oxidation free energy ΔA using the thermodynamic integration (TI) scheme of eq 19 and compared it to the values obtained using eq 2. Intermediate states were generated by running simulations in which the ion was given a fractional charge q varying between 1+ and 3+ in intervals of 0.2. The derivative electrostatic potential $\phi(\mathbf{R}^N)$ of eq 18 was calculated using a finite difference scheme. The system is the same 121 solvent molecule model used to investigate the vertical gap fluctuations (Figures 1 and 2). The plot of the estimate of the thermal average of ϕ as a function of charge q is shown in Figure 4. These potentials were determined by averaging over trajectories of 2 ns for each of the 11 values of q. The potential is perfectly linear in the [+2, +3] interval, yielding, when integrated according to eq 19, an oxidation free energy of $\Delta A_{TI} = -19.70$ eV for the M^{2+}/M^{3+} pair. The agreement with the estimate of $\Delta A_{Marcus} = -19.65$

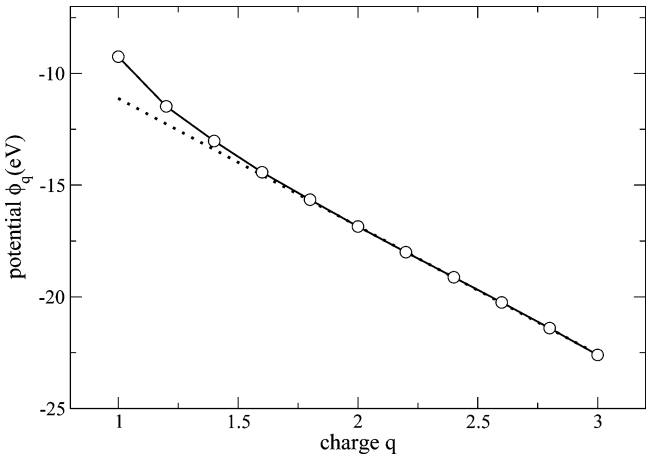

Figure 4. Solvent electrostatic potential (eq 18) at the ion site, $\phi_q(R^N)$, as a function of the charge q of the ion in intervals of 0.2. The dashed line is a linear fit of the 6 data points in the $q = [2,3]$ interval. The extrapolation to the [1,2] interval gives an impression of the deviation from linear response at the lower values of q.

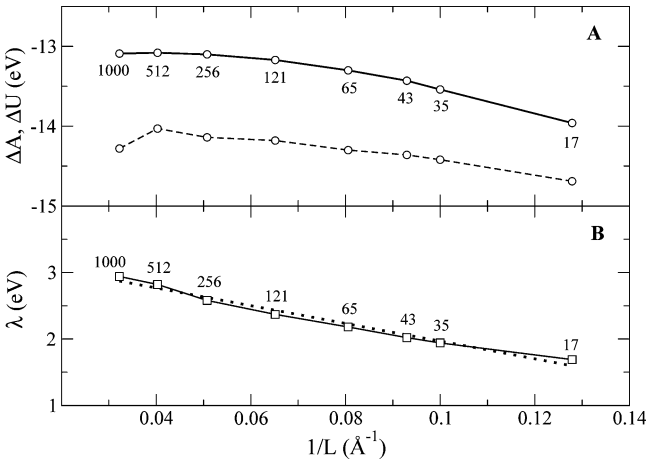

Figure 5. (A) Oxidation free energy ΔA (solid line) and (B) reorganization energy λ for the M^{1+}/M^{2+} pair plotted as a function of the inverse length L of the cubic periodic cell. ΔA and λ have been computed from the time average of the vertical energy gaps such as in Figure 2 according to eqs 2 and 3. The dotted curve in panel A gives the internal energy of oxidation ΔU computed from the difference of the average of total energy. The dotted line in panel B is a linear fit of the λ data points. The intercept at $1/L = 0$ and the slope are given in Table 1. For convenience, the number of solvent molecules contained in the model systems is also indicated.

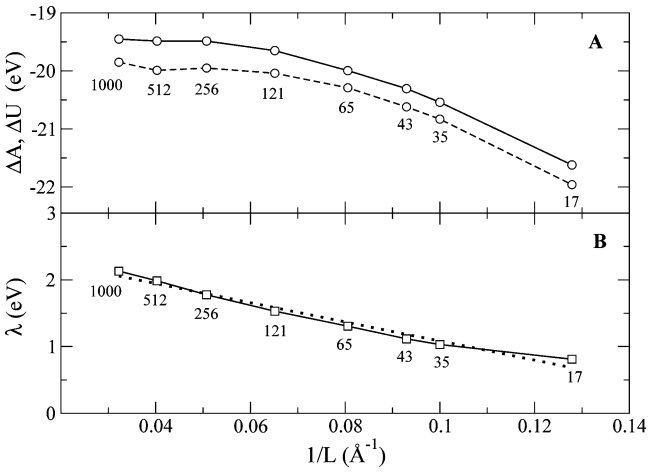

Figure 6. (A) Oxidation free energy ΔA (solid line) and (B) reorganization energy λ for the M^{2+}/M^{3+} pair as computed from the time average of vertical energy gaps (see Figure 5 for further details). The dotted curve in A is the corresponding internal energy of oxidation ΔU.

eV obtained from the vertical gap data of Figure 1 using eq 2 is further evidence that this system is well within the linear regime where Marcus theory applies. The same comparison for the M^{1+}/M^{2+} pair gives as a result $\Delta A_{\text{Marcus}} = -13.17$ eV and $\Delta A_{\text{TI}} = -13.60$ eV, indicating that some discrepancy is beginning to appear between the linear approximation and the in-principle exact thermodynamic integral. This result is consistent with the onset of nonlinear solvent response as manifested in the histograms of Figure 2 and radial distribution functions of Figure 3. What is perhaps somewhat surprising, in view of these energetic and structural data, is that the free energy discrepancies are not so important (less than 5%). Indeed the plot of ϕ displayed in Figure 4 shows only small deviations from linearity around $q = +1$, which means that the linear response approximation demanded by Marcus is satisfied in most of the interval $[+2,+1]$. As also noted before,[19,24,43] eq 2, even though an approximation, is very robust in the sense that it provides a good first estimate of reaction energy, even for systems that are not strictly in the linear regime. The favorable situation, however, breaks down if the interval $[+1,0]$ had been considered, because ϕ is not linear at all in that region as a result of the substantial change in hydration patterns upon neutralization of a solute.

The use of the linear approximation for the reorganization energy in eq 3, outside the regime where linearity strictly applies, is more questionable. Reorganization energy, staying with our example of a simple oxidation half reaction R $\rightarrow$ O, is commonly defined as the amount of free energy required to perturb the solvent from equilibrium in the reactant state (R) to match the equilibrium configuration of the product state (O). For nonlinear systems, the reorganization energies for the forward and reverse reactions (eq 13) are generally different. Equation 3 can be regarded as an estimate of the average of these two reorganization energies, and we can still use the linear approximation to quantify the reorganization. In conclusion, the use of the computationally highly efficient Marcus energy gap relations for the purpose of an analysis of system size dependence seems justified for both the M^{2+}/M^{3+} and M^{1+}/M^{2+} pairs, and this is how the oxidation and reorganization free energies discussed in section 3.2 have been determined.

3.2. Analysis of the Size Dependence of Free Energy. The oxidation free energy ΔA and the reorganization energy λ were computed from the vertical energy gaps according to eqs 2 and 3 for the series of model systems specified in section 2.4, the smallest of which contained 17 water molecules, while the largest contained 1000 water molecules. Figures 5 and 6 show the result for the M^{1+}/M^{2+} and M^{2+}/M^{3+} pairs plotted as a function of $1/L$. The obvious observation to make is that both λ and ΔA are strongly size dependent and that the size dependence is less significant for the M^{1+}/M^{2+} pair (Figure 5), as expected because of the smaller charges of this system.

A closer analysis of Figures 5 and 6 reveals that λ and ΔA have different behaviors with respect to the system size. ΔA increases and effectively reaches an asymptotic value for a system containing 256 water molecules. The asymptotic values are -13.1 eV for the M^{1+}/M^{2+} pair and -19.4 eV for the M^{2+}/M^{3+} pair (asymptotic values are summarized in Table 1). It is clear from these data that the scaling of the size correction for ΔA is supralinear. Note also that the correction is positive. Since solvation free energy is negative, solvation is therefore seemingly *overestimated* by the finite size error in periodic systems. The finite size correction to λ is also positive, and hence the

TABLE 1: Analysis of System Size Dependence of the Oxidation Free Energy ΔA and Reorganization Free Energy λ[a]

reaction	ΔA_∞	$\gamma_{L^{-3}}$	$R_\infty^{\Delta A}$	$R_{L^{-3}}$	λ_∞	$\gamma_{L^{-1}}$	R_∞^{λ}	$\xi_{L^{-1}}$
M^{1+}/M^{2+}	−13.1	−439	1.62	2.20	3.3	−13.3	2.14	−1.85
M^{2+}/M^{3+}	−19.4	−1080	1.82	2.68	2.5	−14.3	2.80	−1.99

[a] A_∞ is the intercept at $1/L^3 = 0$, and $\gamma_{L^{-3}}$ is the slope of a straight line fitted to the computed ΔA values plotted as a function of the inverse volume of the cubic simulation cell of length L (Figure 7). Similarly, λ_∞ is the intercept at $1/L = 0$, and $\gamma_{L^{-1}}$ is the slope of the straight line fitted to the computed λ values plotted as a function of $1/L$ (Figures 5B and 6B). Energies are in units of eV, and lengths are in Å. These intercepts and slopes can be used to derive three different estimates of the born radius as defined by the continuum model of section 2.3, namely, $R_\infty^{\Delta A}$ from A_∞, applying eq 38, $R_{L^{-3}}$ from $\gamma_{L^{-3}}$, applying eq 39, and R_∞^{λ} from λ_∞, applying eq 45. The dimensionless parameter $\xi_{L^{-1}}$ is obtained from $\gamma_{L^{-1}}$ according to eq 47. If the continuum approximation is valid, all three estimates of the cavity radius should give the same number, and $\xi_{L^{-1}}$ should equal the Madelung constant $\xi_{EW} = -2.837$ (for discussion, see section 3.2).

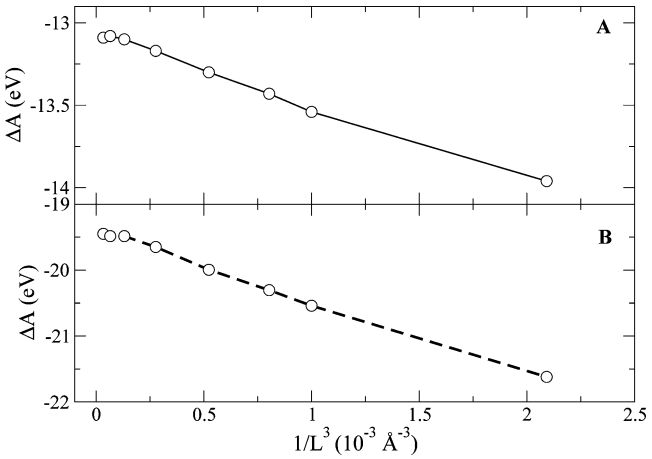

Figure 7. Oxidation free energies ΔA of (A) Figure 5 (M^{1+}/M^{2+} pair) and (B) Figure 6 (M^{2+}/M^{3+} pair) plotted as a function of inverse cell volume $1/L^3$. Intercepts at $1/L^3 = 0$ and slopes of least mean square linear fits are given in Table 1.

reorganization energy is underestimated. In contrast to ΔA, the missing reorganization energy scales with $1/L$, and λ can be smoothly extrapolated to an infinite system limit of 3.3 eV for the M^{1+}/M^{2+} oxidation and 2.5 eV for the M^{2+}/M^{3+} oxidation (see also Table 1).

The λ plots nicely illustrate the extra work that a system has to do to reorient the water molecules far away from the cation when changing charge. The underestimation of reorganization energy can therefore be understood as a direct consequence of the finite size of the system. The overestimation of the solvation free energy, on the other hand, is related to the periodic nature of the system and is due to the net attractive interaction of a charge with its images and neutralizing background (the Wigner lattice energy). The linear dependence of λ on $1/L$ is, moreover, in qualitative agreement with eq 47 derived for the continuum model. The same continuum model predicts for ΔA in a strong polar solvent a scaling with $1/L^3$ (inverse volume). This is the leading term in the $\epsilon \rightarrow \infty$ limit of eq 37, yielding eq 39. This prediction is easily tested by plotting ΔA versus $1/L^3$, as shown in Figure 7. Our data points fairly accurately fit on a straight line, confirming an inverse volume size effect without any clear evidence of crossover to $1/L$ behavior.

For a more quantitative analysis of the reorganization energies of Figures 5B and 6B and the oxidation free energies of Figure 7, we have determined the best straight lines in $1/L$ and $1/L^3$, respectively, fitting these data. The parameters of the linear fits are listed in Table 1. We will first discuss the extrapolation ΔA_∞ of ΔA to infinite system size computed as the intercept with the $1/L^3 = 0$ axis. If the continuum model strictly applies (eq 38), including a cavity radius R, which is independent of oxidation state, ΔA_∞ of the M^{2+}/M^{3+} oxidation should be a factor of $5/3 = 1.67$ larger than ΔA_∞ for M^{1+}/M^{2+}. The ratio we find for the simulation results is 1.48, which is smaller but not by too much. More serious is the discrepancy for the infinite size limits λ_∞. According to eq 45, these values should be the same, while the extrapolated λ_∞ for the M^{1+}/M^{2+} reaction is 0.8 eV larger compared to that for M^{2+}/M^{3+}. The 0.8 eV larger reorganization energy for the reaction with lower charge can be rationalized by attributing it to the inner sphere reorganization, which is more prominent for this reaction, as discussed in section 3.1.

Perhaps even more important than the question of variation of cavity radius with oxidation state is the question whether the radius for the reaction free energy and the reorganization energy can be taken to be the same. Therefore, we compared the two estimates of cavity radius R that can be derived from ΔA_∞ and λ_∞ using eqs 38 and 45, respectively. The numbers are given in Table 1 as $R_\infty^{\Delta A}$ and R_∞^{λ}. Ideally, the values of these cavity radii should coincide. This is of course expecting too much. Indeed, we find that $R_\infty^{\Delta A}$ is significantly smaller than R_∞^{λ}. Comparison to the radial distribution functions of Figure 3 shows that $R_\infty^{\Delta A}$ is similar to the ionic radius ($\lesssim$2Å), while our values for R_∞^{λ} are more characteristic for the size of an ion plus the first solvation shell as measured by the radius where the coordination number adds up to 6 ($\gtrsim$2.2Å, depending on oxidation state). The small value of $R_\infty^{\Delta A}$ is not unreasonable because ΔA represents the full interaction of the ion and the aqueous solvent, including the tightly bound first hydration shell. There is a general consensus that the reorganization for the iron-like model system is "outer sphere", meaning that it is dominated by the long-range orientational polarization of the solvent. The contribution of relaxation of the first solvation shell is minor, which makes it plausible that the radius of the coordination complex would be a more suitable measure of the cavity relevant for the reorganization. Our relative values for R_∞^{λ} and $R_\infty^{\Delta A}$ are consistent with this picture.

It is possible to obtain a third independent estimate of cavity radius, namely, from the slope of the linear dependence of ΔA on $1/L^3$ using eq 39. This is the radius most important to us because of its possible application in a finite size correction to the AIMD estimates of ΔA. It is therefore interesting to see that the results for this radius, indicated by $R_{L^{-3}}$ in Table 1, are closer to R_∞^{λ} than to $R_\infty^{\Delta A}$. Recalling our argument about what causes the size effect in λ, the similarity between $R_{L^{-3}}$ and R_∞^{λ} suggests that the mechanism determining the leading finite size correction to the oxidation free energy is controlled by the perturbation of the solvent structure due to the constraints imposed by the periodic boundary conditions. Can we say the same about the slope of λ against $1/L$? According to eq 47, this coefficient (multiplied by 2) is in the continuum approximation given by the cubic Madelung constant $\xi_{EW} = -2.84$ and is therefore independent of the charge or radius of the ion. Our value, referred to as $\xi_{L^{-1}}$ in Table 1, is $\sim$2.0. The accuracy of the calculation is sufficient to make this 30% deviation significant, a claim that is also supported by the good agreement between the values for the two oxidation reactions we have studied (Table 1). This suggests that there is a further long-range effect $\sim 1/L$ that is not described by a linear dielectric

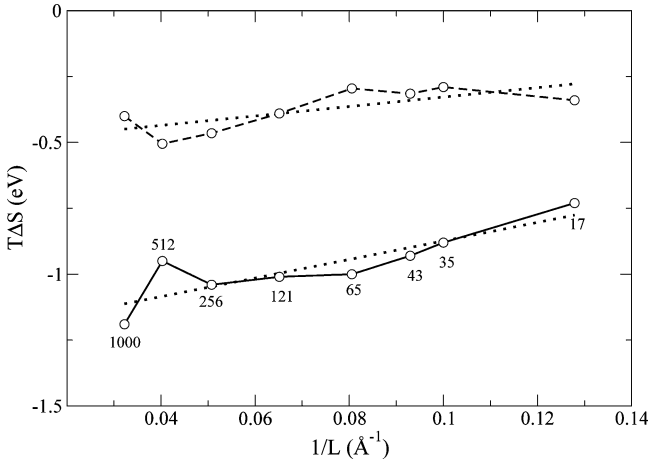

Figure 8. Entropy change represented as $T\Delta S$ as a function of $1/L$ for the M^{1+}/M^{2+} (solid curve) and M^{2+}/M^{3+} (dashed curve) oxidation. $T\Delta S$ values have been computed as the difference between the total internal energy ΔU and free energy ΔA changes of Figure 5 and Figure 6. Statistical uncertainties for the larger systems are on the order of 10% (0.15 eV). The dotted lines are linear fits used in the analysis of the entropy in section 3.3. The $1/L = 0$ intercepts are -1.22 and -0.51 eV. The corresponding slopes are 3.5 and 1.8 eV Å.

continuum. We have, at this stage, no clear idea of what this could be. A possibility is electrostriction. The interpretation of elastic effects is, unfortunately, seriously complicated by the constraint on volume in our calculations. To resolve this issue, further work is needed. A first priority is repeating the simulations under conditions of constant pressure.

3.3. Entropy Effects. With an estimate of the reaction free energy ΔA available, the entropy change can be computed, in principle, from the difference of the total energy change ΔU and ΔA. ΔU can be obtained directly by evaluating the average difference of total energy of the M^{n+}(aq) and $M^{(n+1)+}$(aq) trajectories. These averages have also been included in Figures 5 and 6. The curves for ΔA and ΔU are almost parallel. Evidently, size dependence is largely an enthalpic effect. The resulting estimates of $T\Delta S$ are plotted in Figure 8. The deterioration of the statistics with increasing L is due to the well-known difficulty of obtaining converged results for total energy differences of large systems (in contrast to free energy differences, which are computed from analytical derivatives). We first note the sign of the entropy change, which is negative, indicating that increase in positive charge due to oxidation leads to a decrease in entropy. This is in agreement with experiment and is often explained in terms of the structure-making effect of high charge ions compared to ions with lower charges. The idea is that a high ionic charge enhances the network structure in the liquid, thus decreases the entropy.

Of particular interest in the present context is, again, the finite size correction. The entropy change induced in the solvent by the cation appears to be short-range. However, the accuracy of the results for entropy in Figure 8 is not sufficient to rule out a weak dependence on size. For further analysis, we therefore again resort to a comparison to the prediction of continuum theory. Differentiation of the free energy of eq 35 with respect to temperature should give, in principle, (minus) the entropy created by the charging of the ion. Assuming, as is the rule, that the cavity radius R is invariant with temperature, temperature enters only through the static dielectric constant ϵ. However, extreme caution is needed. The failure of dielectric continuum models to describe entropy is generally accepted (see, for example, ref 30). If, in spite of this warning, we go ahead and write the thermal derivative of the Born free energy change of eq 38 as

$$\Delta S_B = \frac{{q_O}^2 - {q_R}^2}{2\epsilon R}\left(\frac{1}{\epsilon}\frac{\partial \epsilon}{\partial T}\right) \approx -\frac{\Delta A_B}{\epsilon}\left(\frac{1}{\epsilon}\frac{\partial \epsilon}{\partial T}\right) \qquad (48)$$

and substitute the experimental value of the temperature coefficient of the dielectric constant of water at room temperature ($\epsilon^{-1}\partial\epsilon/\partial T = -0.0046$ K^{-1}), we find $T\Delta S = 0.017\Delta A_B$. For the M^{2+}/M^{3+} pair, using the value of ΔA_∞ of Table 1, this gives $T\Delta S \approx -0.3$ eV, which is surprisingly, and probably fortuitously, close to the estimate of $\Delta S \approx -0.5$ obtained from Figure 8. Indeed the continuum model is already in trouble for the M^{1+}/M^{2+} oxidation. The (absolute) value of the entropy change for this reaction, as given in Figure 8, is about 0.7 eV larger compared to that for M^{2+}/M^{3+}, whereas it should be a factor 3/5 smaller according to the continuum model. In the framework of (microscopic) Marcus theory, however, this difference of 0.7 eV can be viewed as a quantitative measure of the contribution of the inner sphere (first coordination shell) rearrangement accompanying the M^{1+}/M^{2+} oxidation as mentioned earlier. The sign is also correct if we can interpret the more structured OM radial distribution function (Figure 3) of M^{2+} compared to M^{1+} as an increase in order and therefore a decrease in entropy. We should bear in mind, though, that because of the active role of the first solvation shell in M^{+1}/M^{2+} oxidation, the linear approximation, which is the basis for all our thermodynamical calculations, is less accurate for this system. The rather subtle entropy results may be more sensitive to these errors than the free energy changes.

If we next compute the size correction by differentiating eq 37 to temperature,

$$\Delta S_L - \Delta S_B = \frac{{q_O}^2 - {q_R}^2}{\epsilon}\left[\frac{\xi_{EW}}{2L} + \frac{2\pi R^2}{3L^3}\right]\left(\frac{1}{\epsilon}\frac{\partial \epsilon}{\partial T}\right) \qquad (49)$$

we recover an $1/L$ term that seems to be in conflict with the simulation results. As mentioned, the statistics of the data in Figure 8 is, however, rather poor, and one could maintain that the dependence of $T\Delta S$ is approximately linear after all, which would lead to a derivative (slope) of 1.8 eV Å for the M^{3+}/M^{2+} oxidation and about 3.5 eV Å for M^{2+}/M^{1+}. The linear coefficients computed from eq 49, using the experimental values of the dielectric constant and temperature derivative, are 6.2 eV Å and 3.8 eV Å, respectively. First of all, the sign is correct (which seems to already be an issue for entropy derived from continuum theory[30]). Also, the actual values, while clearly not in agreement, are of comparable magnitude considering the uncertainties. From this we tentatively conclude that our results for the entropy change show a weak $1/L$ dependence on system size, which would also be consistent with our interpretation of the $1/L$ contribution to the solvent reorganization discussed in section 2.3.

4. Summary and Concluding Remarks

Provided the response of the solvent to a change of charge of a solvated ion is approximately linear, the corresponding free energy change can be computed directly from the vertical ionization energy in the reactant and product state. This highly efficient and robust numerical method, derived from the Marcus theory of ET, was exploited to investigate the system size dependence of oxidation free energy for an iron-like aqueous cation using a classical SPC force field model. We also

computed the reorganization energy for the (half) reaction using the same approach. The model systems contain only a single ion plus a varying number of water molecules. Cubic periodic boundary conditions are applied with long-range interactions computed using the Ewald system. For this type of system, Hummer et al.[51] concluded that the interaction between the ion, its periodic images, and the neutralizing background (the Wigner lattice energy) is compensated ("screened") by the polarization of the solvent with the result that the finite system size correction to the solvation free energy effectively scales, not with inverse cell length $1/L$ as one might expect, but with inverse cell volume $1/L^3$. Our calculations of oxidation free energy confirm this observation. The $1/L$ dependence was, however, recovered in the computation of the finite size correction to the reorganization energy. This result is also, at first, somewhat of a paradox, because reorganization energy, unlike oxidation free energy, compares free energies of systems with the same charge, and the contribution of the Wigner energy should cancel. This led us to interpret the $1/L$ dependence of the finite size error of reorganization energy as further support for the Hummer hypothesis, because it shows that the perturbation of the solvent polarization induced by the presence of the periodic array of ions also scales with $1/L$, which is a necessary condition if it is to compensate the Wigner energy of the ions.

The paper also returned to the periodic generalization of the Born continuum model for ion solvation introduced by Hummer and co-workers[52] and studied again by Hünenberger.[58] Using the same model, we derived the corresponding expression for the reorganization energy, which confirmed the $1/L$ dependence of the leading finite size correction for this quantity. The combined continuum approximations for oxidation and reorganization energy, when used to fit the simulation results, yield three different estimates of the Born cavity radius. We found that the radius derived from the infinite size extrapolation of reorganization energy is significantly larger than the corresponding radius for the oxidation free energy (0.5−1 Å depending on the charge of the ion). The third value of the cavity radius, controlling the inverse volume term in the expression of the oxidation free energy, was found to be closer to the larger radius for reorganization energy.

This observation about the prefactor determining the magnitude of the inverse volume term is the most relevant result for the understanding of the size dependence (and ultimately the design of a finite size correction) for our AIMD calculations of redox free energies. This formed the main motivation for the present study. We regard the results of the classical simulation as encouraging from this practical perspective. They provide further insight in the conditions under which the argument of compensating errors applies, which we used to justify the modest system sizes used in the AIMD calculation of redox potentials. For the errors to cancel in full redox reactions, not only must the charges of reactant and product be equal (eq 5), but the effective solvation radii must also match. The relevant solvation radius, we propose, is related to the solvent reorganization. Clearly, what is needed to corroborate these conclusions is further data on ions with different charge, particularly anions, as well as larger solute species, particularly molecules. This will be the subject of future research.

Acknowledgment. Jochen Blumberger and Ruth Lynden-Bell are acknowledged for their helpful comments. R.A. is grateful to the Spanish government (MEC) and the Marie Curie Fellowship program for financial support.

References and Notes

(1) Hynes, J. T. *Annu. Rev. Phys. Chem.* **1985**, *36*, 573.
(2) Nitzan, A. *Chemical Dynamics in Condensed Phases*; Oxford University Press: Oxford, 2006.
(3) Marcus, R. A. *J. Chem. Phys.* **1956**, *24*, 966.
(4) Marcus, R. A. *J. Chem. Phys.* **1956**, *24*, 979.
(5) Marcus, R. A. *J. Chem. Phys.* **1957**, *26*, 867.
(6) Marcus, R. A. *J. Chem. Phys.* **1965**, *43*, 679.
(7) Marcus, R. A.; Sutin, N. *Biochim. Biophys. Acta* **1985**, *811*, 265.
(8) Marcus, R. A. *Rev. Mod. Phys.* **1993**, *65*, 599.
(9) Lee, S.; Hynes, J. T. *J. Chem. Phys.* **1988**, *88*, 6853.
(10) Kim, H. J.; Hynes, J. T. *J. Chem. Phys.* **1990**, *93*, 5194.
(11) Kim, H. J.; Hynes, J. T. *J. Chem. Phys.* **1990**, *93*, 5211.
(12) Kim, H. J.; Hynes, J. T. *J. Chem. Phys.* **1992**, *96*, 5088.
(13) Newton, M. D.; Friedman, H. L. *J. Chem. Phys.* **1988**, *88*, 4460.
(14) Liu, Y.-P.; Newton, M. D. *J. Phys. Chem.* **1994**, *98*, 7162.
(15) Tachiya, M. *J. Phys. Chem.* **1993**, *97*, 5911.
(16) Matyushov, D. V. *J. Chem. Phys.* **2004**, *120*, 7532.
(17) Warshel, A. *J. Phys. Chem.* **1982**, *86*, 2218.
(18) Hwang, J. K.; Warshel, A. *J. Am. Chem. Soc.* **1987**, *109*, 715.
(19) King, G.; Warshel, A. *J. Chem. Phys.* **1990**, *93*, 8682.
(20) Olsson, M. H. M.; Hong, G.; Warshel, A. *J. Am. Chem. Soc.* **2003**, *125*, 5025.
(21) Kuharski, R. A.; Bader, J. S.; Chandler, D.; Sprik, M.; Klein, M. L.; Impey, R. W. *J. Chem. Phys.* **1988**, *89*, 3248.
(22) Carter, E. A.; Hynes, J. T. *J. Phys. Chem.* **1989**, *93*, 2184.
(23) Carter, E. A.; Hynes, J. T. *J. Chem. Phys.* **1991**, *94*, 5961.
(24) Zhou, H.-X.; Szabo, A. *J. Chem. Phys.* **1995**, *103*, 3481.
(25) Yelle, R. B.; Ichiye, Y. *J. Phys. Chem. B* **1997**, *101*, 4127.
(26) Ando, K. *J. Chem. Phys.* **1997**, *106*, 116.
(27) Ando, K. *J. Chem. Phys.* **2001**, *114*, 9470.
(28) Hartnig, C.; Koper, M. T. M. *J. Chem. Phys.* **2001**, *115*, 8540.
(29) Small, D. W.; Matyushov, D. V.; Voth, G. A. *J. Am. Chem. Soc.* **2003**, *125*, 7470.
(30) Ghorai, P. K.; Matyushov, D. V. *J. Phys. Chem. A* **2006**, *110*, 8857.
(31) Leontyev, I. V.; Tachiya, M. *J. Chem. Phys.* **2005**, *123*, 224502.
(32) Halley, J. W.; Hautman, J. *Phys. Rev. B* **1988**, *38*, 11704.
(33) Benjamin, I. *J. Phys. Chem.* **1991**, *95*, 6675.
(34) Rose, D. A.; Benjamin, I. *J. Chem. Phys.* **1994**, *100*, 3545.
(35) Rose, D. A.; Benjamin, I. *Chem. Phys. Lett.* **1995**, *234*, 209.
(36) Straus, J. B.; Voth, G. A. *J. Phys. Chem.* **1993**, *97*, 7388.
(37) Straus, J. B.; Calhoun, A.; Voth, G. A. *J. Chem. Phys.* **1995**, *102*, 529.
(38) Calhoun, A.; Koper, M. T. M.; Voth, G. A. *J. Phys. Chem. B* **1999**, *103*, 3442.
(39) Hartnig, C.; Koper, T. M. *J. Am. Chem. Soc.* **2003**, *125*, 9840.
(40) Car, R.; Parrinello, M. *Phys. Rev. Lett.* **1985**, *55*, 2471.
(41) Tateyama, Y.; Blumberger, J.; Sprik, M.; Tavernelli, I. *J. Chem. Phys.* **2005**, *122*, 234505.
(42) Blumberger, J.; Sprik, M. *Theor. Chem. Acc.* **2006**, *115*, 113.
(43) Blumberger, J.; Tavernelli, I.; Klein, M. L.; Sprik, M. *J. Chem. Phys.* **2006**, *124*, 064507.
(44) VandeVondele, J.; Lynden-Bell, R.; Meijer, E. J.; Sprik, M. *J. Phys. Chem. B* **2006**, *110*, 3614.
(45) VandeVondele, J.; Sulpizi, M.; Sprik, M. *Angew. Chem., Intl. Ed.* **2006**, *45*, 1936.
(46) Ayala, R.; Sprik, M. *J. Chem. Theory Comput.* **2006**, *2*, 1403.
(47) Sulpizi, M.; Raugei, S.; VandeVondele, J.; Carloni, P.; Sprik, M. *J. Phys. Chem. B* **2007**, *11*, 36969.
(48) Tateyama, Y.; Blumberger, J.; Ohno, T.; Sprik, M. *J. Chem. Phys.* **2007**, *126*, 204506.
(49) VandeVondele, J.; Ayala, R.; Sulpizi, M.; Sprik, M. *J. Electroanal. Chem.* **2007**, *607*, 113.
(50) Blumberger, J.; Bernasconi, L.; Tavernelli, I.; Vuilleumier, R.; Sprik, M. *J. Am. Chem. Soc.* **2004**, *126*, 3928.
(51) Hummer, G.; Pratt, R. L.; Garcia, A. E. *J. Phys. Chem.* **1996**, *100*, 1206.
(52) Hummer, G.; Pratt, L. R.; Garcia, A. E. *J. Chem. Phys.* **1997**, *107*, 9275.
(53) Hummer, G.; Pratt, L. R.; Garcia, A. E. *J. Phys. Chem. A* **1998**, *102*, 7885.
(54) Hummer, G.; Pratt, L. R.; Garcia, A. E.; Shekhar, G. *J. Phys. Chem. B* **1998**, *102*, 3841.
(55) Figuerido, F.; Del Buono, G. S.; Levy, R. *J. Phys. Chem. B* **1997**, *101*, 5622.
(56) Lynden-Bell, R. M.; Rasaiah, J. C. *J. Chem. Phys.* **1997**, *107*, 1981.
(57) Bogusz, S.; Cheatham, T. E., III; Brooks, B. R. *J. Chem. Phys.* **1998**, *108*, 7070.
(58) Hünenberger, P. H.; McCammon, J. A. *J. Chem. Phys.* **1999**, *110*, 1856.
(59) Baker, N. A.; Hünenberger, P. H.; McCammon, J. A. *J. Chem. Phys.* **1999**, *110*, 10679.

(60) Peter, C.; van Gunsteren, W. F.; Hünenberger. *J. Chem. Phys.* **2003**, *119*, 12205.
(61) Kastenholz, M. A.; Hünenberger, J. *J. Chem. Phys.* **2006**, *124*, 224501.
(62) Leslie, M.; Gillan, M. J. *J. Phys.: Condens. Matter* **1985**, *18*, 973.
(63) Makov, G.; Payne, M. C. *Phys. Rev. B* **1995**, *51*, 4014.
(64) Schultz, P. A. *Phys. Rev. Lett.* **2000**, *84*, 1942.
(65) Schultz, P. A. *Phys. Rev. Lett.* **2006**, *96*, 246401.
(66) Lento, J.; Mozos, J.-L.; Nieminen, R. M. *J. Phys.: Condens. Matter* **2002**, *14*, 2637.
(67) Wright, A. F.; Modine, N. A. *Phys. Rev. B* **2006**, *74*, 235209.
(68) Tachiya, M. *J. Phys. Chem.* **1989**, *93*, 7050.
(69) Kirkwood, J. G. *J. Chem. Phys.* **1935**, *3*, 300.
(70) VandeVondele, J.; Sprik, M. *Phys. Chem. Chem. Phys* **2005**, *7*, 1363.
(71) Berendsen, H. J. C.; Postma, J. P. M.; van Gunsteren, W. F. V.; Hermans, J. In *Intermolecular Forces: Proceedings of the Fourteenth Jerusalem Symposium on Quantum Chemistry and Biochemistry*; Pullman, B., Ed.; Reidel: Dordrecht, The Netherlands, 1981; p 331.
(72) Allen, M. P.; Tildesley, D. J. *Computer Simulation of Liquids*; Oxford University Press: Oxford, 1987.
(73) Smith, W.; Forester, T. R. *DL_POLY 2.14*; Council for the Central Laboratory of the Research Councils, Daresbury Laboratory: Warrington WA4 4AD, England, 2003.